DOI: 10.24874/ti.1552.09.23.01

Tribology in Industry

www.tribology.rs

RESEARCH

Effects of Adding Graphite to Epoxy Resin on its Mechanical Properties and Mild-to-Severe Wear Performance at its Heat Distortion Temperature

K.Y. Eayal Awwad[a,*]

[a]*Mechanical Engineering Department, Faculty of Engineering, Tafila Technical University, Tafila 66110, Jordan.*

Keywords:

Graphite
Epoxy
Tribology
Mechanical properties
Heat distortion temperature

* Corresponding author:

K. Y. Eayal Awwad
E-mail: K.awwad@ttu.edu.jo

Received: 19 September 2023
Revised: 27 November 2023
Accepted: 3 January 2024

A B S T R A C T

In this study, epoxy/graphite composites were fabricated based on different weight fractions (0, 3, 6, and 9 wt.%) of graphite powder for bearing applications. The mechanical and tribological properties were assessed. Adhesive wear tests covered the severe regions, where the interface temperature (IFT) exceeded the heat distortion temperature (HDT) of the epoxy. Graphite additions improved elastic modulus and hardness but decreased fracture strain and toughness of the composites. The tribological behaviors in the mild wear region were improved as the graphite content increased. In the mild wear region, the increase in graphite additions showed a good improvement by reducing the specific wear rate (SWR) and coefficient of friction (COF). In the severe wear region, the neat epoxy and higher graphite concentrations exhibited a dramatic increase in SWR, whereas the lowest addition of 3 wt.% exhibited good wear performance. For epoxy, the reason was that IFT exceeded its HDT, while the aggregation of graphite particles was the main reason in the case of higher graphite concentrations. SEM examinations showed severe wear signs—high ploughing and fracture—when IFT exceeded the HDT. However, by reducing the IFT, graphite additions did not show such severe wear features due to the accelerated heat dissipation.

1. INTRODUCTION

Polymeric composites are increasingly being used to replace traditional materials in a variety of engineering, automotive, aviation, and industrial applications. This might be traced mostly to their unique properties, which include, but are not limited to, a high strength-weight ratio, corrosion resistance, being inexpensive, and being easy to fabricate [1]. With regards to tribological applications, polymer composites exhibited high performance in such applications [1–3]. Therefore, there is an increasing trend to replace tribo-components that are based on metals, such as bushings, bearings, and gears, with polymer-based materials. Several polymers are utilized in tribological applications, including epoxy, polyether ether ketone (PEEK), and polytetrafluoroethylene (PTFE) [4]. However, in their pristine forms, polymers are not often used

in applications for tribology enhancement since the great majority of pure polymers possess an elevated coefficient of friction and limited wear resistance [2]. To address this issue, polymers are commonly modified to fulfil the specific demands of tribological applications. This is normally achieved by techniques like coatings, fiber reinforcement, and the inclusion of fillers [1, 2].

Solid-lubricant fillers are widely used to reduce the coefficient of friction (COF) of polymers owing to their easy-to-fragment structure, which forms an interfacial boundary lubrication layer. They are mainly classified into two groups: (1) organic lubricants, such as PTFE and Polychlorotrifluoroethylene (PCTFE); and (2) inorganic lubricants, which include graphene, graphite, tungsten disulfide (WS_2), and molybdenum disulfide (MoS_2) [5]. Numerous investigations have been conducted to examine their effects on the COF and specific wear rate (SWR) of various kinds of polymers, such as WS_2/PEEK [6], graphite/ABS [7], and graphite/ phthalazinone ether sulfone ketone (PPESK) [8]. These studies showed a positive impact of such fillers on enhancing the tribological properties of polymers, resulting in a noticeable reduction in both the SWR and COF. However, in wear processes, the thermal energy generated at the interface, where rubbing occurs, has a substantial influence on the wear characteristics of the polymers. The generated frictional heat expedites the wear rate when the interface temperature (IFT) exceeds the specific polymer's temperatures, such as heat distortion temperature (HDT) and glass transition temperature (T_g) [9–11]. Due to this factor, the performance of most solid lubricants is restricted to polymer-specific temperatures. The thermal conductivity (TC) of polymers is critical for the wear resistance. The high TC results in superior service performance [1,12].

The TC of polymers with low specific temperatures needs to be modified, which prolongs the working temperature ranges. In other words, the reduction in COF can be easily achieved by various kinds of solid lubricants. However, the lubrication efficiency is restricted to working temperatures below the range of the specific polymer's temperatures, i.e., HDT and T_g. For example, Ye et al. [13] studied the effect of MoS_2 addition on the fretting wear of novolac epoxy. The findings indicated that both the wear rate and COF were significantly reduced. To prevent MoS2 oxidation, which could reduce its lubricating efficacy, monitor the IFT by reducing sliding distance and/or load. Similar results were reported for PTFE [14] and WS_2 [6] lubricants. The limited working temperature range is mostly due to reduced TC in most solid lubricant-modified polymers. For instance, the TC of PTFE is 0.2–0.3 W/(m.K) [15], in the range of epoxy's value, 0.2 W/(m·K) [16]. As a result, such solid-lubricant fillers do not affect polymer TC. Hence, their usage is limited under the thermo-mechanical stresses of wear processes. Polymers with low TC can be modified by using fillers with higher TC.

Attempts are sometimes made to enhance the TC of polymers through various treatments or coatings for specific applications in which the thermal properties have pivotal effects. It is expected that the heightened TC of a selected filler will enhance the wear characteristics of polymers by improving the heat dissipation process from the contacting surfaces. The effectiveness of such an impact will be seen more in the severe regions than in the mild regions of the wear process. It should be thoroughly studied. Within this context, carbon-based lubricants, which include graphene and graphite, are quite suitable for tribological applications due to their capability to improve not only the self-lubricating properties but also the TC of polymers. For instance, the TC of graphite is in the 200 –2000 W/(m·K) range [17], at least 1,000 times that of epoxy. Relevant studies showed the high capability of graphite fillers to improve the TC of polymers [17] and potentially improve their specific temperatures, such as T_g [18].

In the literature, some research has been published on the lubricating efficiency of graphite/polymer systems [7, 8]. Experiments on the lubrication efficiency of such fillers mainly covered the mild wear regions; however, the severe wear regions in which the IFT reaches the polymers' specific temperatures, i.e., HDT, are rarely reported so far. Many open questions surrounding the wear mechanism of such fillers at the critical IFT and their tribological behaviors must be answered. The impact of filler concentration on the SWR and COF, the influence of fillers on heat dissipation, and the wear mechanism are still open questions. It is worthwhile to investigate

the tribological properties of epoxy/graphite composites. In this study, epoxy/graphite composites are developed utilizing variant weight fractions of graphite fillers (0, 3, 6, and 9 wt.%). The mechanical characteristics and tribological behaviors of the produced composites have also been investigated.

2. MATERIALS AND METHODS

2.1 Materials

In this study, epoxy resin R246TX (opaque liquid, specific gravity of 1.10 g/ml at 25 °C, and viscosity of 900–1100 mPas at 25 °C) and H160 hardener (clear pale brown liquid, specific gravity of 30.0 g/ml at 25 °C, viscosity of 0.95 mPas at 25 °C, and pot life of 120 min for 100g at 25 °C) were used as a base-matrix composite, which was purchased from ATL Composites Pty Ltd., Australia. The resin-to-hardener mixing ratio is 4:1. The HDT of the pure epoxy is 65 °C after post-curing at 100 °C for 4 h, as given in the technical data sheet provided by the supplier. Graphite powder, provided by Sigma-Aldrich Pty Ltd., Australia, with an average particle size of less than 20 μm, was used as a solid lubricant filler.

2.2 Sample preparation

Figure 1 illustrates a comprehensive representation of the sample preparation methodology. For the pure epoxy, the hardener was gradually added to the epoxy resin. For epoxy-graphite composites, a specific weight fraction of 0, 3, 6, and 9 wt.% of graphite powder was incrementally added to the epoxy resin. The graphite masses were precisely weighed using a high-accuracy balance of 1×10^{-5} g. After that, the mixture was continuously stirred for 2 minutes at 250 rpm using an electrical mixer. The stirring speed was chosen to be low to avoid excessive heat. The mixtures were degassed in a vacuum-sealed oven chamber at -70 kPa and 50°C for 30 min to eliminate air bubbles. The mixture was promptly poured into the designated steel molds. The steel molds were prefabricated from AISI D2 steel with specified cavities to produce the tensile and wear samples. For tensile testing, the dog-bone samples were manufactured in conformity with ASTM D638-99 [19]. The thickness of the samples is 8 mm, and the total length is 190 mm. The gauge length located on the narrow section is 80 mm. The overall width is 20 mm, while the width of the narrow section is 10 mm. Regarding the wear test samples, the mold has a cavity with a length, width, and height of 58×20×25 mm, respectively, designed to fit the block-on-ring (BOR) tribometer in accordance with the ASTM G77-98 standard [20]. The mixtures were self-cured by maintaining them inside the molds at 25 °C for 24 h and then post-cured at 100 °C for 4 h. Following the full curing process, epoxy and its composites were subjected to mechanical and tribological testing. The epoxy/graphite composites, with varying concentrations of graphite, are denoted by "epoxy-Gr-x" where x is the weight fraction of graphite.

2.3 Mechanical and adhesive wear testing

The mechanical properties of epoxy and its composites were evaluated through hardness and tensile tests. Tensile testing was performed using the MTS 810 TestStar with a load capacity of 10 KN in compliance with ASTM D638-99 [19]. The head speed during the tensile test was constant at 1 mm/min for all examined samples. For each composite, three samples were tested, obtaining the average values. The Shore D hardness of the composites was measured according to ASTM D2240 [21]. From each sample, three readings were obtained to get the average readings. The tribological behaviours of the neat epoxy and epoxy/graphite composites were conducted using a BOR tribometer in conformity with the ASTM G77-98 standard [20]. The selection of wear test settings was determined based on the compatibility of the block materials, i.e., epoxy and its composites, with the intended applications [11,22,23]. Since there are many applications where steel parts slide against polymer composites, it is necessary to explore the wear mechanism between the hard steel and the soft epoxy composite materials. In this study, the SWR and COF of the tested samples were obtained under variant wear conditions due to the variation of the applied load.

The wear experiments were conducted under dry contact conditions at ambient temperature, with relative humidity ranging from 40% to 50%. The velocity of sliding was consistently held at 1 m/s, while the magnitude of the applied forces was 15, 30, 50, and 70 N.

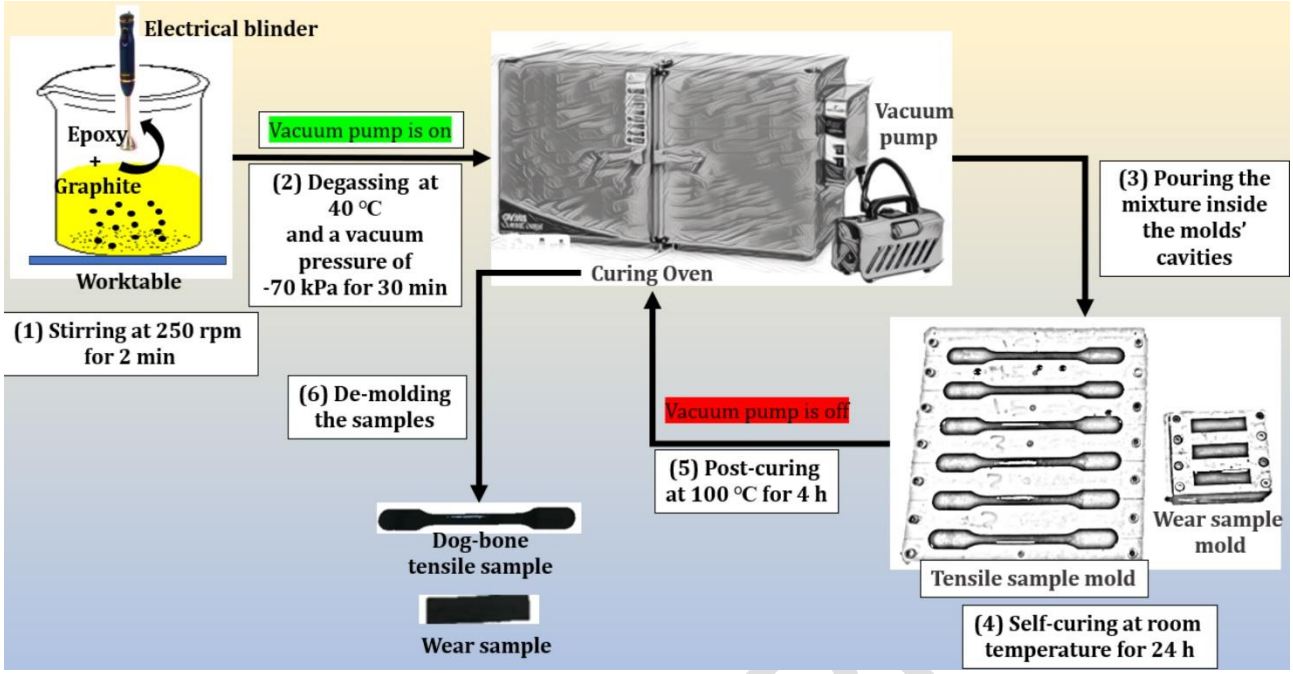

Fig. 1. Schematic representation of the sample preparation process for epoxy composites.

The pressure-velocity (PV) product values of these parameters exhibited fluctuations ranging from 0.35 to 0.60 MPa.m/s. This range falls within the allowable range for bearing applications [11,22,23]. It is noteworthy to note that the contact pressure (P) was determined in the steady-state region using finite element modelling.

The sliding distance of the wear tests was 12 km, allowing the wear to transfer from the running-in stage into the steady-state stage. The setup of the BOR tribometer is depicted in Fig. 2. The fixed wear samples, blocks, were slid against a rotating stainless steel counterface (AISI 304, hardness = 1,250 HB, average roughness of Ra = 0.2 µm, and diameter = 228 mm). The tangential friction force was recorded by the friction load cell, which was affixed to the load lever. This data was collected using a data acquisition system.

Before starting each wear test, the targeted surfaces of the wear samples and stainless-steel ring were polished, ensuring a surface roughness of ≥ Ra = 0.2 µm. A mobile surface-roughness tester, MarSurf M 400, was used to measure the Ra values of the steel ring and the worn surfaces. To remove suspended particles, the worn surfaces were cleaned using acetone-soaked soft tissue paper. The specimens were air-dried before weighing to evaluate the weight loss via a mass scale with a precision of 1×10^{-5} g. After measuring the mass loss, the worn volume was calculated based on the mass loss and the corresponding density of each composite. SWR values in (mm^3/N.mm) were basically calculated based on the following relationship:

$$SWR = \Delta V / (L \times F_N)$$

where ΔV is the volume loss during the test duration, F_N is the load, and L is the total sliding distance. To ensure data repeatability and reproducibility, a minimum of three repetitions were conducted for each experiment. The IFT was measured using a thermal imaging camera, the Testo 876.

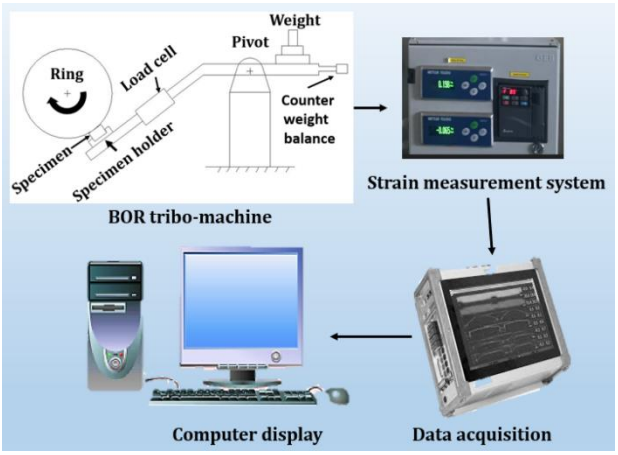

Fig. 2. Illustration of the setup of wear tests.

2.4 Scanning electron microscopy (SEM) analysis

To deeply understand the influence of graphite on the mechanical characteristics, wear, and frictional behaviours of epoxy. SEM device type JEOL JCM-6000 BENCHTOP was utilized to analysis surfaces of tensile and wear samples. To increase the examined surfaces' conductivities, a JEOL Smart Coater-ion Sputtering Device was used, which coated these surfaces with a thin gold layer. It is worthwhile to mention here that the morphology of the wear samples for all tested materials in this study was spotted in the normal zone of the BOR wear profile, as defined by the recent study conducted by K. Y. Eayal Awwad et al. [24].

3. RESULTS AND DISCUSSION

3.1 Mechanical properties of the composites

The addition of graphite additives significantly altered the mechanical properties of epoxy and caused morphological changes. The effect of graphite concentrations on the modulus of elasticity (E) and the fracture strength of epoxy is illustrated in Fig. 3.

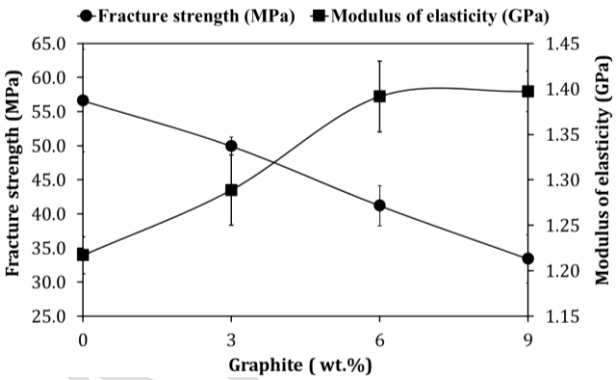

Fig. 3. The effect of varying concentrations of graphite on fracture strength and modulus of elasticity of epoxy.

The mechanical properties of the neat epoxy are consistent with previous research [11,16]: fracture strength ranges from 58 to 94 MPa, whereas the modulus of elasticity ranges from 0.6 to 2.7 GPa. The modulus of elasticity displayed a positive proportional relationship with graphite concentration, yielding a maximum value of 1.4 ± 0.02 GPa for the epoxy-Gr-9 composite, corresponding to a 15% increase as compared to that of neat epoxy. In contrast, the graphite additions negatively influenced the fracture strength, while the neat epoxy exhibited a maximum value of 56.62 ± 7.52 MPa. Compared to neat epoxy, the 9 wt.% graphite inclusions reduced the fracture strength by 41%. Similarly, fracture strain and fracture toughness exhibit the same trend of fracture strength, as seen in Fig. 4 (a and b). However, the shore D hardness of epoxy (see Fig. 4 (c)) improved marginally with increasing graphite concentration. For instance, adding 9 wt.% of graphite somewhat enhanced the hardness value by 10% when compared to neat epoxy.

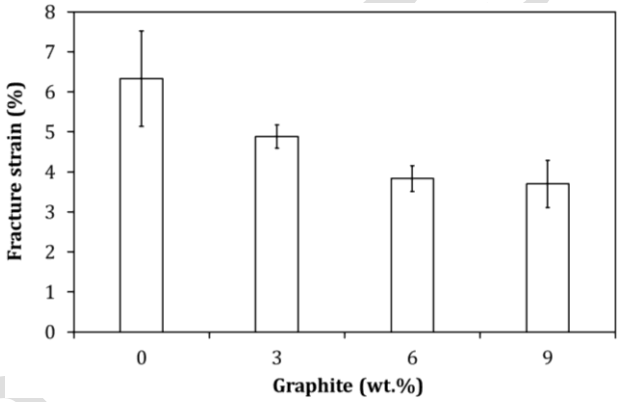

(a) Fracture strain

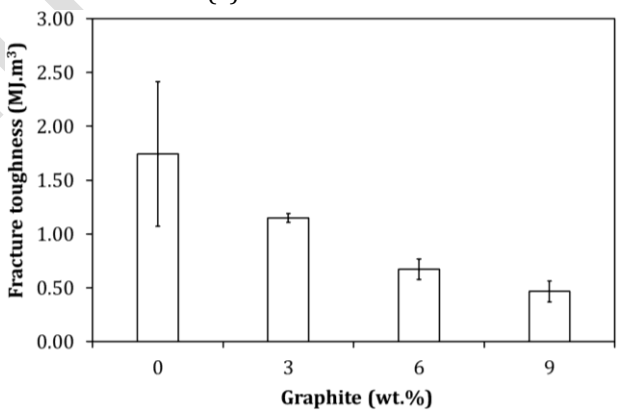

(b) Fracture toughness

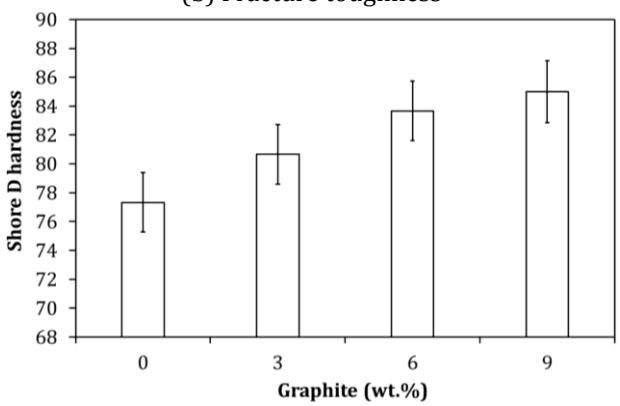

(c) Shore D hardness

Fig. 4. The influence of varying graphite amounts on the mechanical characteristics of epoxy: (a) Fracture strain, (b) fracture toughness, and (c) shore D hardness.

Comparable findings were documented in different kinds of polymers, such as epoxy/graphene nanoplatelets [11] and phthalonitrile/silicon carbide [25]. Improvements in modulus of elasticity and hardness could be attributed mostly to the brittle nature of graphite, which has a stiffness value of around 600 GPa [26]. Because the used graphite is unfunctionalized, the epoxy structure, including its crosslinked density, does not change. [27]. Similar findings were reported for other polymers, such as ultra-high molecular weight polyethylene (UHMWPE) [28] and PEEK [27].

Figure 5. presents the SEM micrographs of the fractured surfaces of the tensile samples, which support a further explanation of the fracture mechanism of the epoxy and epoxy/graphite composites. The stretched river-like pattern on the neat epoxy indicates stretching marks, as shown in Fig. 5(a). The fractured surface of the neat epoxy samples exhibited signs of cleavage failure and stretching. These features are typical for the neat epoxy, as indicated by its notably high values of fracture strain and fracture toughness, as shown in Fig. 4 (a and b). Increasing graphite concentration reduces the deformation of the epoxy matrix in their vicinity; hence, increasing the concentration is expected to result in progressively brittle behaviour, as indicated by the squamous-like pattern, as shown in Figs. 5 (c and b). The presence of a higher concentration of graphite resulted in enhanced visibility of the squamous-like morphology.

The primary factor contributing to a decrease in fracture strength is the phenomenon of particle aggregation and agglomeration. These phenomena significantly reduce the interaction between the particles of the filler and the polymer matrix, thereby functioning as a stress concentrator inside the matrix. It is worth mentioning that π−π interactions and Van der Waals forces between graphite layers primarily cause particle aggregation, making the polymer dispersion inside the matrices difficult [29,30]. Furthermore, the exothermic heat of the reaction assists in the agglomeration of graphite particles by decreasing the viscosity of the epoxy matrix. Furthermore, the appearance of embrittlement phases, which are indicated by a squamous-like pattern (see Fig. 5 (c and d)), decreases the fracture strength of polymers [31].

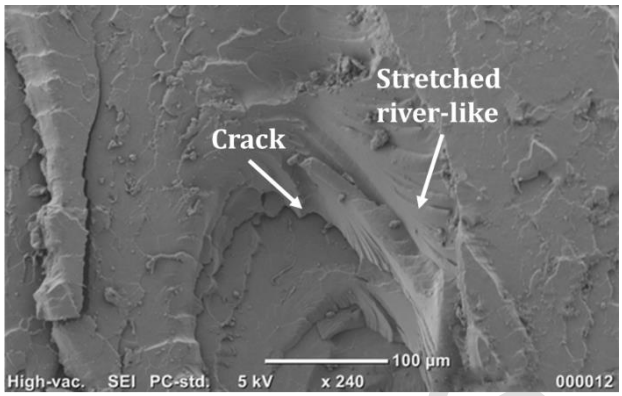

(a) Neat epoxy

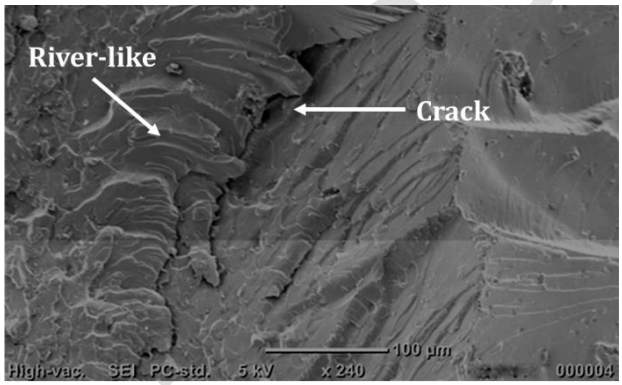

(b) Epoxy-Gr-3

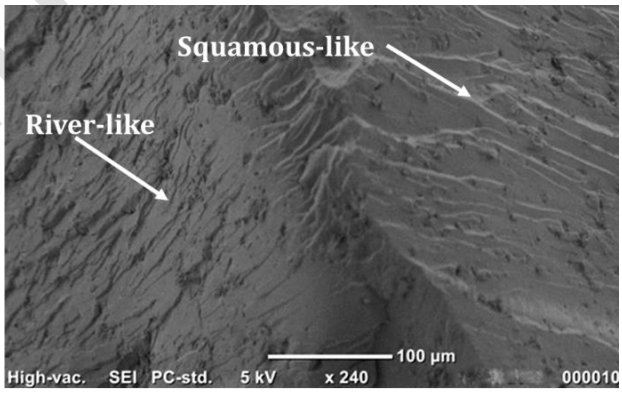

(c) Epoxy-Gr-6

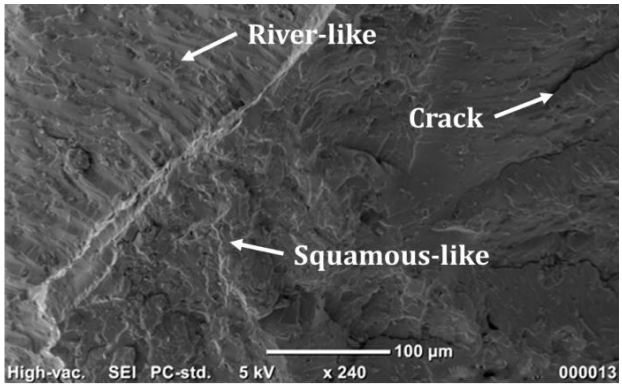

(a) Epoxy-Gr-9

Fig. 5. SEM images of the fractured surfaces of the tensile samples: (a) neat epoxy, (b) epoxy-Gr-3, (c) epoxy-Gr-6, and (d) epoxy-Gr-9.

Brittleness restricts the chain mobility of the molecular motion, resulting in a reduction in fracture strain and fracture toughness [32]. A similar observation was reported by Atif et al. [33], which stated that a filler concentration of more than 1 wt.% mostly reduces the fracture strength, fracture strain, and fracture toughness of epoxy composites. It is noteworthy that the filler's nature plays a crucial role in the mechanical properties of polymers. Some fillers can enhance fracture strain and toughness. For instance, Yu et al. [34] studied the effect of nano-rubber particles on the fracture toughness of epoxy. It was noticed that the increase in the nano-rubber particles significantly improved the fracture toughness of the epoxy matrix. This was mostly because the rubber particles can absorb elastic energy during the shear stresses accompanied by drawing and tearing, which contrasted with the low absorption capabilities of graphite fillers. It is worth noting that all composites did not show signs of manufacturing defects such as bubbles and voids. This is mostly due to the efficiency of mixing and degassing during the samples' preparation process.

3.2 Tribological properties of the composites

The wear tests were conducted under dry-adhesive conditions, employing various loads of 10, 30, 50, and 70 N over a sliding distance of 12 km. Fig. 6 illustrates the impact of these loads on the SWR of epoxy composites. The lowest value of SWR was observed when a load of 30 N was applied to both composites and neat epoxy. This value was even lower than the SWR observed, with the lowest applied load being 10 N. This can be attributed to the suitable generated heat under this load, which helps to initiate a thin viscoelastic layer. This layer serves a pivotal function in mitigating crack propagation when subjected to fatigue stresses [11,35]. Nevertheless, when exceeding 30 N, the accompanying thermo-mechanical stresses increase, resulting in a transition from a mild to a severe wear region, as indicated by high SWR values in the cases of 50 N and 70 N. Similar trends were exhibited by epoxy/graphene nanoplatelets [11] and polyester/graphite-cotton [36].

The graphite additions exhibited a beneficial effect on epoxy's wear resistance. This is observable in the case of low applied loads, as in the cases of 10 N and 30 N. The improvement is due to the inherent self-lubrication capability of graphite, which manifests in the creation of a stable transfer film, resulting in a significant decrease in the SWR values. For instance, in the case of 30 N, the 9 wt.% of graphite reduced the SWR value by 47% as compared to the SWR of neat epoxy. At the lower range of applied load, it is clearly observed that there is no considerable reduction in SWR by increasing the graphite content above 3 wt.%. The addition of 9 wt.% graphite exhibited only a slight reduction of 7% in SWR as compared to the epoxy-Gr-3 composite. At high applied loads, i.e., 50 N and 70 N, SWR increased for both neat epoxy and its composites. Surprisingly, by increasing the applied load, the higher content of graphite exhibited higher values of SWR. The SWR trend, at high applied loads, of neat epoxy is similar to the trends of epoxy-Gr-6 and epoxy-Gr-9 composites; however, the reasons may be completely different. To gain a better understanding of these behaviours, it is imperative to consider the mechanical properties and specific epoxy's temperatures, as the wear process involves a combination of thermo-mechanical stresses.

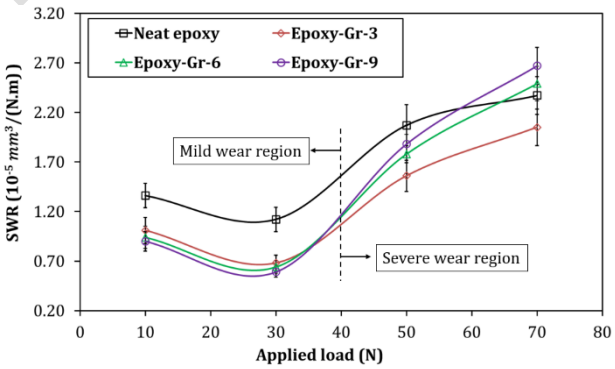

Fig. 6. The influence of applied loads on the specific wear rate (SWR) of epoxy and epoxy-Gr composites.

SWR versus the sliding distance of 12 km under all different loads is shown in Figs. 7 and 8. It was evident that there was an observable match between the 10 N and 30 N cases for epoxy and its composites, as shown in Fig. 7. SWR started with high values and subsequently decreased as the sliding distance increased. This behaviour is due mainly to the BOR tribometer's configuration, in which the contact area is minimum, and the contact pressure is maximum at the starting point, resulting in a high rate of material removal, i.e., a high SWR.

This stage is known as the running-in stage [9,11]. Following that, an increase in the sliding distance increased the contact area between the rubbing surfaces, which lowered the contact pressure and, therefore, reached the steady-state stage, i.e., the steady-state value of SWR [11]. Regarding the impact of variant concentrations of graphite on the SWR of epoxy, there is an observable reduction in the SWR with the increase of the graphite additions under the low applied loads of 10 and 30 N, as discussed earlier (see Fig. 6 (a and b)).

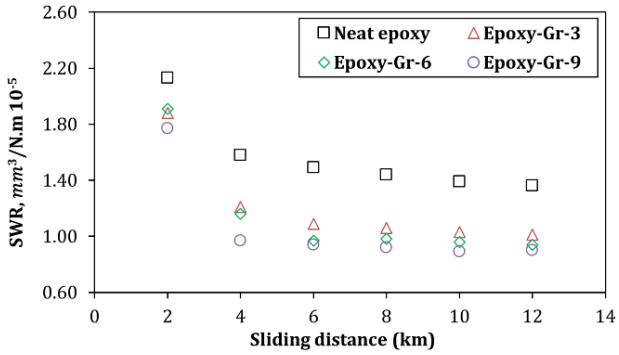

(a)

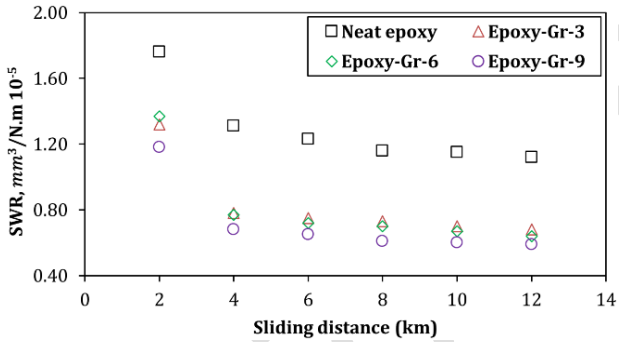

(b)

Fig. 7. The variation of specific wear rate (SWR) over the sliding distance for epoxy and its composites at mild loads of (a) 10 N and (b) 30 N. The standard deviation values for all readings ranged between (0.06 to 0.28).

In the case of the high applied loads of 50 N and 70 N, the effect of the running-in stage for approximately the first 4 km of sliding distance can also be noted, as shown in Fig. 8. Nevertheless, these high applied loads exhibited different trends as compared to the steady-state stage in the cases of 10 N and 30 N of applied loads. Regarding the neat epoxy, the increase in SWR values, shown in Fig. 8, was mainly due to the fact that IFT has exceeded the epoxy's HDT, which is 65 °C. Accordingly, the molecule bonding of epoxy resin will be broken, reducing load-bearing capacity under thermo-mechanical stresses [11,37,38]. On the other hand, all epoxy-Gr composites did not reach the HDT under all applied loads. This is mainly attributed to the capability of graphite to enhance the TC and the specification's temperature of epoxy, as reported by relevant studies [26,39].

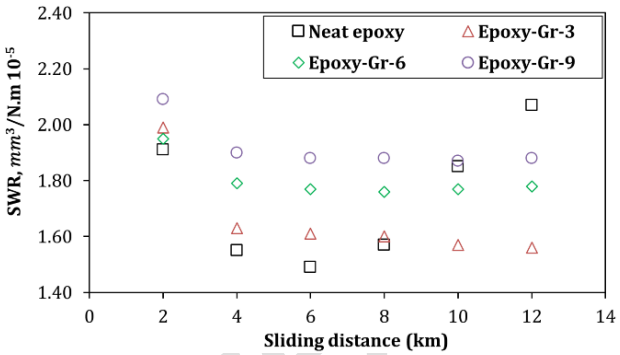

(a)

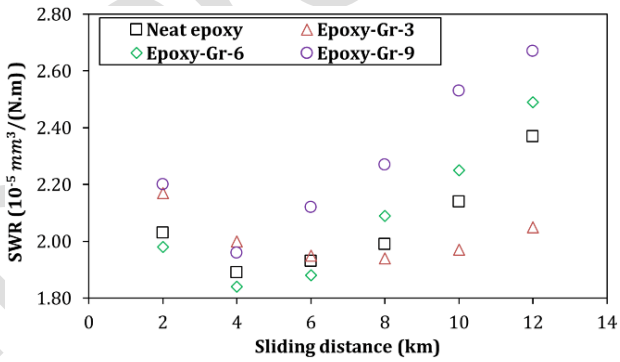

(b)

Fig. 8. The variation of specific wear rate (SWR) over the sliding distance for epoxy and its composites at higher loads of (a) 50 N and (b) 70 N. The standard deviation values for all readings ranged between (0.11to 0.27).

The improvement in the TC leads to an increase in the dissipation heat rate from the rubbing surfaces. At high loads of 50 N and 70 N, the low content of graphite, i.e., 3 wt.%, exhibited lower values of SWR compared to the high graphite content of 6 and 9 wt.% (see Fig. 8). The reason behind that could be summarized as follows: (1) The increase in graphite content is generally accompanied by a significant reduction in toughness (see Fig. 4(b)), which causes the epoxy to become more brittle and more prone to fatigue fracture, especially when subjected to high applied loads [11,40]. (2) The increase in graphite concentrations increases the agglomeration and aggregation of graphite particles, thus diminishing the thermal and mechanical characteristics of epoxy. Consequently, the tribological properties of polymers are adversely affected [35,39].

The friction behaviours of epoxy and its composites are presented in Figs. 9-11. The influence of variant concentrations of graphite on the COF of epoxy under mild applied loads is shown in Fig. 9. It can be seen in Fig. 9 (a and b) that when low applied loads of 10 N and 30 N are utilized, the COF curves exhibit a relatively smoother behaviour within the stable range values for the neat epoxy. This contrasts with the COF curves obtained under high applied loads of 50 N and 70 N, as depicted in Fig. 10 (a and b).

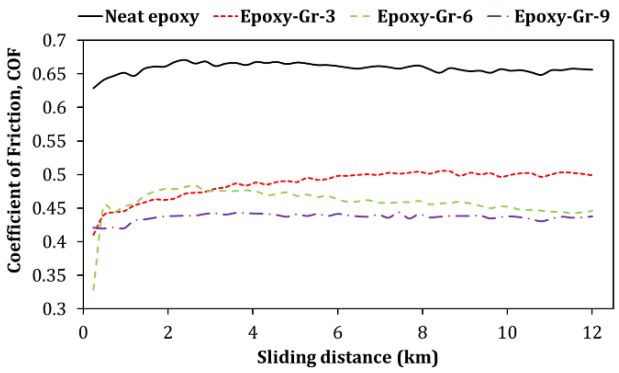

(a)

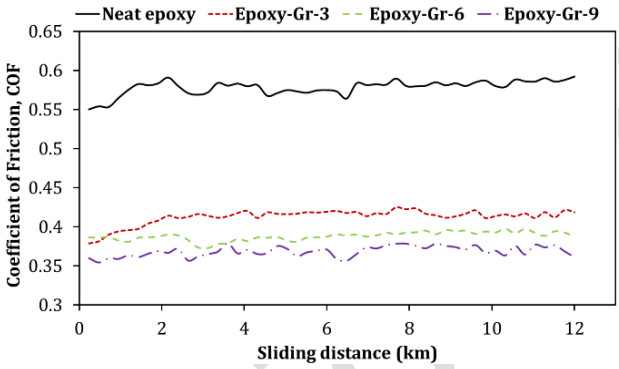

(b)

Fig. 9. Coefficient of friction (COF) over the sliding distance of epoxy and epoxy-Gr composites at mild applied loads of (a) 10N and (b) 30N.

HDT serves as the primary and crucial factor influencing the behaviours observed under these high loads. The COF curves for neat epoxy demonstrated an abrupt rise after 6 km and 4 km under loads of 50 N and 70 N, respectively. The common factor behind the sudden change in COF in both cases is that the IFT exceeded the HDT of epoxy at 65 °C. Even though HDT is below T_g, once the IFT exceeds HDT, the molecular bonding of the matrix resin may become weak and thus easy to break [11,37,38,41], particularly when subjected to the high mechanical stresses associated with the wear process. This is also the primary reason for the drastic increase in the SWR, as discussed previously. A relevant study by Tahir et al. [42] investigated the influence of working temperature on the tribological behaviours of carbon fibre epoxy composite. It was noticed that increasing the working temperature rapidly increased the COF due to the development of frictional heat, which can weaken the epoxy matrix's bonding. Analogous findings have been revealed on glass fibre epoxy composites by Arikh and Gohil [41]. Liu et al. [38] conducted a study to explore the HDT effect on the wear resistance of phenolic/nylon-graphene composites. The findings showed that there is a positive correlation between the HDT and the level of wear resistance that can be achieved.

In all cases, it is evident that the inclusion of graphite powder has a beneficial effect on reducing the COF of epoxy, as shown in Figs. 9 and 10. For instance, the minimum reduction achieved of 26% was recorded in the case of 3 wt.% of graphite addition, epoxy-Gr-3, under an applied load of 10 N. The reason for this is primarily due to the self-lubricating properties of the lubricant. During the sliding process, the graphite particles detach and are then trapped on the worn surface of the worn sample, creating a stable transfer film. This layer acts as a lubrication film between the rubbing surfaces, resulting in a significant reduction in COF values. This behaviour is linked to the lamellar structure of graphite, in which the layers are assembled within a hexagonal-unit cell. The interlayer bonds are predominantly governed by Van der Waals forces and are fragmented when subjected to shear stresses during the sliding process [5]. All epoxy-Gr composites exhibited signs of stable transfer film under all loads. Similar observations were reported on various polymers, such as graphite/ABS [7] and graphite/PPESK [8].

The stick-slip phenomenon was observed in the case of neat epoxy, especially at the higher applied loads, as indicated by the observable fluctuation in COF, as shown in Fig. 10 (a and b). This is mainly attributed to the low self-lubricating properties of neat epoxy [43]. In contrast, the COF fluctuation in the case of epoxy-Gr composites was very minor during the wear process. The reason for that is that adding graphite significantly improved the self-lubricating properties of epoxy [43].

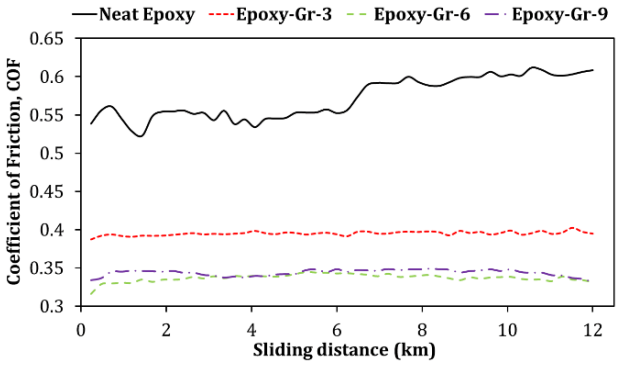

(a)

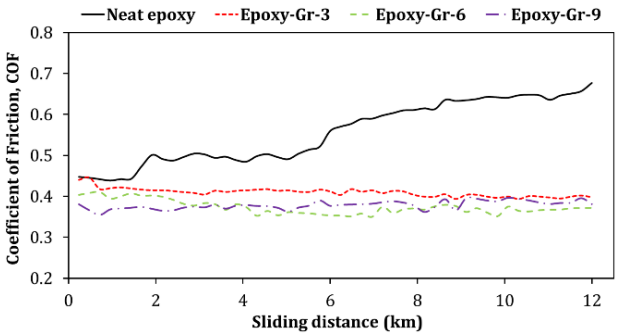

(b)

Fig. 10. Coefficient of friction (COF) over the sliding distance of epoxy and epoxy-Gr composites at higher applied loads of (a) 50N and (b) 70N.

The impact of the different applied loads on the COF of epoxy and epoxy-Gr composites is depicted in Fig. 11. When the load increased, the COF decreased. The frictional force at the interface intensifies because of the increased applied load. Accordingly, the viscoelastic film and the transfer film will be created in the case of neat epoxy and epoxy-Gr composites, respectively. The creation of these films is further influenced by the IFT and, thus, the applied load. Analogous behaviours in other polymer composites have been found, such as polyester [36] and PPESK [8].

In contrast to metallic materials, the wear behaviour of polymers is notably affected by the generated heat due to the rubbing process. The main cause of this sensitivity is the relatively poor thermal conductivities, which are very low as compared to metals. The low TC of polymers imposes restrictions on their allowable operating temperatures in tribological applications, in which temperature is a crucial factor [1,38]. This obstacle was one of the main motivations of the current study, wherein the used solid-lubricant material has a high potential to enhance the TC of polymers.

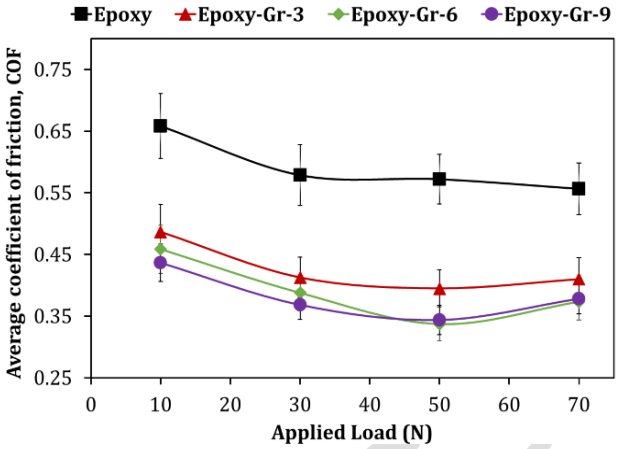

Fig. 11. The influence of loads on the average coefficient of friction of epoxy and epoxy-Gr composites.

Fig. 12 exhibits the effect of graphite additions on the IFT at high applied loads: 50 N (Fig. 12(a)) and 70 N (Fig. 12(b)). It is worth mentioning here that the interface temperatures in cases of low applied loads were below the HDT of epoxy.

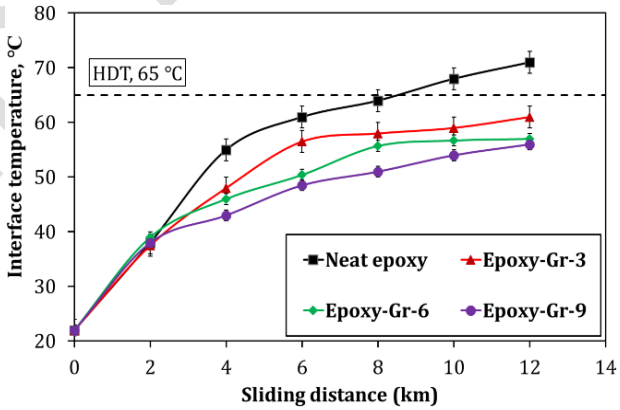

(a)

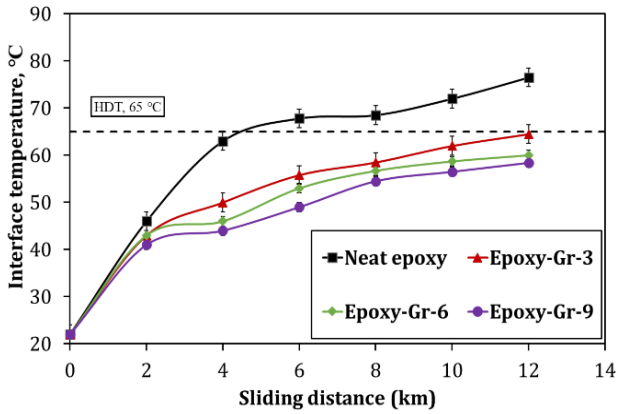

(b)

Fig. 12. Interface temperature (IFT) vs. the sliding distance for epoxy and epoxy-Gr composites, under higher applied loads; (a) 50 N and (b) 70 N.

The increase in sliding distance raises the IFT. The highest recorded IFT attained by the neat epoxy was 76.5 °C at 70 N. It can be noticed that the IFT exceeded the HDT, 65 °C, after 8 km in the case of 50 N and after 4 km in the case of 70 N. As discussed above, it was noticed that when the IFT exceeds the HDT, both COF and SWR dramatically increase, exceeding the HDT and leading to weak bonds [38,41]. As a result, there will be a reduction in the elastic modulus of epoxy, which will lead to a reduction in its load-bearing capacity. The load effect on the IFT of epoxy and epoxy-Gr composites after 12 km is depicted in Fig. 13. The lower IFT when compared to the neat epoxy is proof that the addition of graphite increased the efficiency of the heat dissipation process. This resulted from the beneficial influence of graphite on the TC of epoxy.

A relevant study by Wang et al. [39] was conducted to investigate graphite's effect on epoxy's TC. For instance, adding 4.5 wt.% of expended graphite significantly enhanced the TC of epoxy by about 440% compared to the neat epoxy. Herein, the reduction achieved on IFT was low compared with the expected improvement in the TC of epoxy. The maximum reduction in IFT of about 24% is attained for the epoxy-Gr-9 composite in the case of 70 N of applied load. One probable explanation is that heat dissipation depends on the area of contact, which is tiny in the case of a BOR configuration. Another factor could be attributed to the agglomeration of graphite particles, which reduces the thermal properties of the epoxy matrix [26,39].

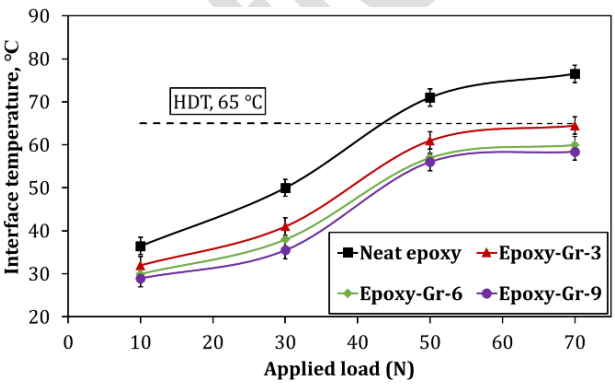

Fig. 13. Interface temperature (IFT) vs. the applied load for epoxy and epoxy-Gr composites.

Fig. 14 displays various thermal images of the epoxy and its composites under the applied load of 70 N. The morphology of the worn surfaces of epoxy and its composites was examined using SEM.

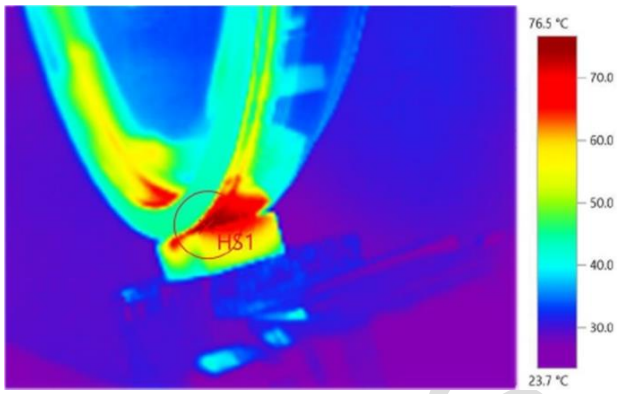

(a) Neat epoxy

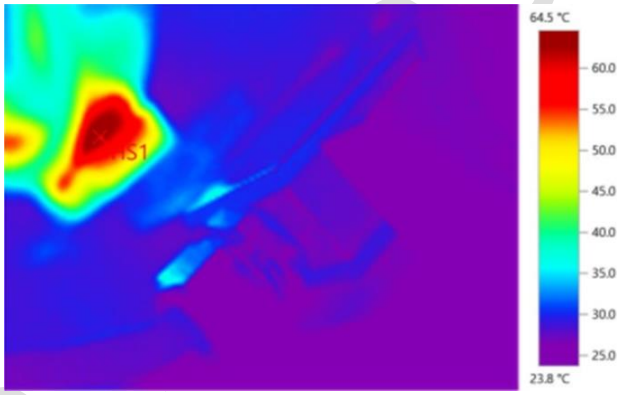

(b) Epoxy-Gr-3

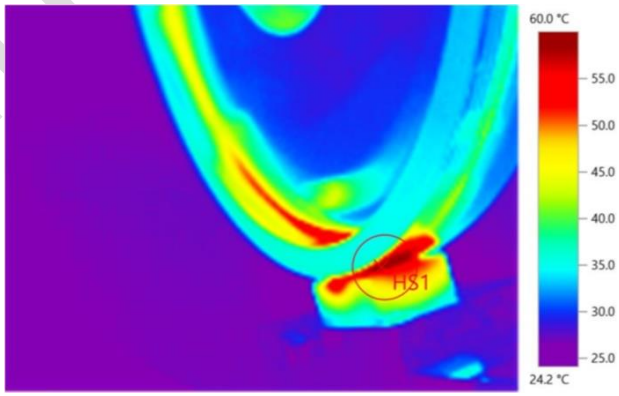

(c) Epoxy-Gr-6

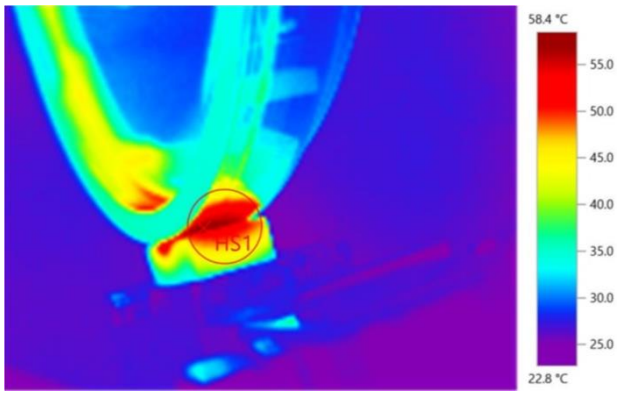

(d) Epoxy-Gr-9

Fig. 14. Thermal images for epoxy and its composites during the wear process before almost completing the full sliding distance of 12 km under applied loads of 70 N.

The load effect on the morphology of the neat epoxy is presented in Fig. 15. At the low applied load of 10 N (see Fig. 15(a)), the worn surface was exposed to abrasive wear dominated by signs of the cold raptures, which were in the form of crazes. The reasons behind this morphology could be mainly attributed to the lower interface temperature under low applied loads. Moreover, the brittle nature of the epoxy matrix promotes such features under shear stresses during the rubbing process. In contrast, the SEM micrograph of the neat epoxy in the case of 30 N (Fig. 15(b)) exhibited stretched signs with smooth deformation. This is in good agreement with the SWR values, which were lower than the values of 10 N; see Fig. 6. The wear mechanism may start with the abrasive wear mode due to the low IFT. As the IFT increases during the wear process, the wear mechanism converts to the adhesive wear mechanism, which can explain the morphology of smooth deformation.

The higher applied loads of 50 N and 70 N produced a smashed morphology with severe wear features manifested by signs of high ploughing and fractures, as shown in Fig. 15 (c and d). The wear mechanism of the neat epoxy under high applied loads starts with abrasive wear mode and eventually turns to adhesive wear mode due to the increase in the IFT. The wear mechanism was accompanied by stick-slip phenomena at the beginning of the process due to the low self-lubricating properties of neat epoxy [43]. This phenomenon was also observed during the wear process due to the increase in IFT, as indicated by the sharp fluctuation of COF, as shown in Fig. 10 (a and b). This explains the high SWR values obtained under these loads. Severe wear signs resulted from the high thermal and mechanical stresses that were exerted on the worn surfaces. The main key factor is the IFT; practically, when it exceeds the HDT of epoxy, it results in weakened bonds in the epoxy matrix [38,41]. This emphasized the importance of heat dissipation to avoid such severe wear mechanisms. Eventually, these morphologies comply with SWR, COF, and surface roughness findings. Similar findings were reported on, carbon/epoxy composites [42], and epoxy/graphene composites [11].

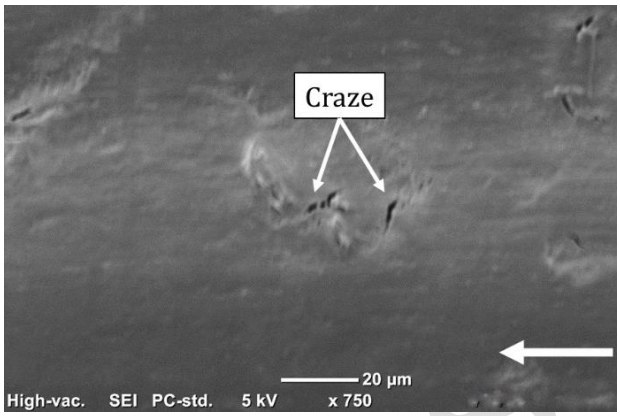

(a) 10N

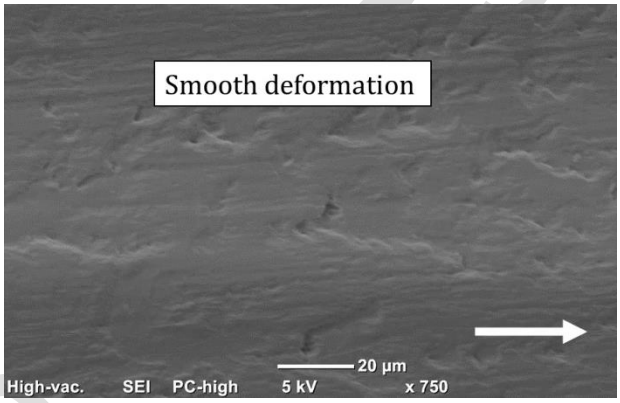

(b) 30N

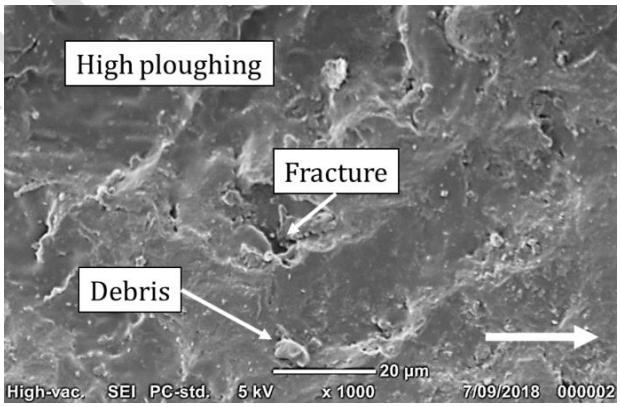

(c) 50N

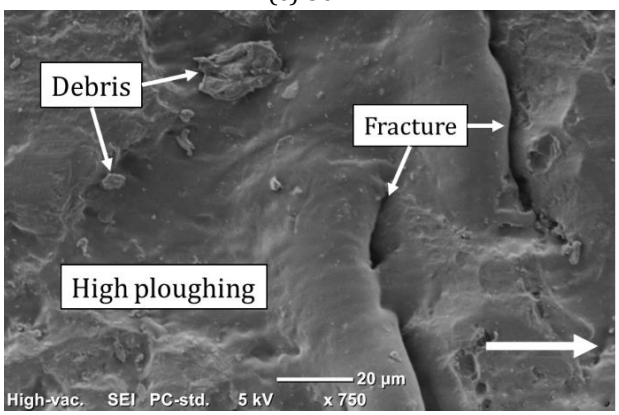

(d) 70N

Fig. 15. SEM images of the worn surfaces of neat epoxy under variant loads. The arrows on the bottom-right corner indicate the sliding direction of the ring.

The higher applied loads of 50 N and 70 N produced a smashed morphology with severe wear features manifested by signs of high ploughing and fractures, as shown in Fig. 15 (c and d). The wear mechanism of the neat epoxy under high applied loads starts with abrasive wear mode and eventually turns to adhesive wear mode due to the increase in the IFT.

The wear mechanism was accompanied by stick-slip phenomena at the beginning of the process due to the low self-lubricating properties of neat epoxy [43]. This phenomenon was also observed during the wear process due to the increase in IFT, as indicated by the sharp fluctuation of COF, as shown in Fig. 10 (a and b). This explains the high SWR values obtained under these loads. Severe wear signs resulted from the high thermal and mechanical stresses that were exerted on the worn surfaces. The main key factor is the IFT; practically, when it exceeds the HDT of epoxy, it results in weakened bonds in the epoxy matrix [38,41]. This emphasized the importance of heat dissipation to avoid such severe wear mechanisms. Eventually, these morphologies comply with SWR, COF, and surface roughness findings. Similar findings were reported on carbon/epoxy composites [42], and epoxy/graphene composites [11].

The main purpose of the inclusion of graphite filler as a solid-lubricant material is to reduce the COF and SWR. Fig. 16 shows the SEM images of epoxy and epoxy-Gr composites at a load of 30 N after 12 km. Compared to epoxy, it can be clearly noticed the presence of a transfer film in the case of epoxy-Gr composites, as shown in Fig. 16(b, c, and d). The creation of the stable-transfer film justifies the substantial reduction in the values of COF attained through the inclusion of graphite. In addition, the transfer film functions as a protective film that covers the worn surface, resulting in a reduction in the rate of wear [8,11].

It can be noticed that the increase in graphite concentration results in a relatively thicker layer. However, it is important to note that the increase in graphite concentration is accompanied by the existence of wear debris, as shown in Fig. 16(d). This is mainly due to the agglomeration and aggregation phenomena of graphite particles inside the epoxy matrix, which increase as the graphite concentration increases.

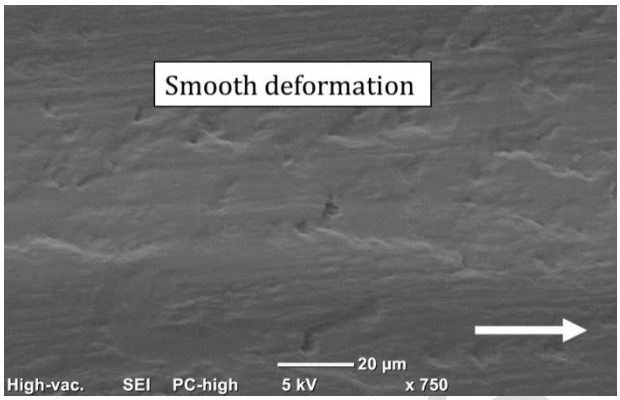

(a) Neat epoxy

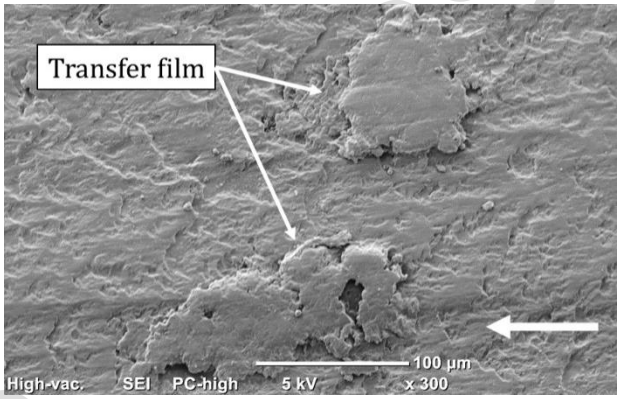

(b) Epoxy-Gr-3

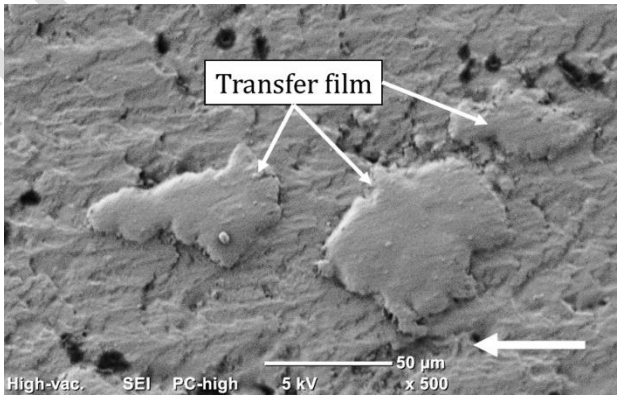

(c) Epoxy-Gr-6

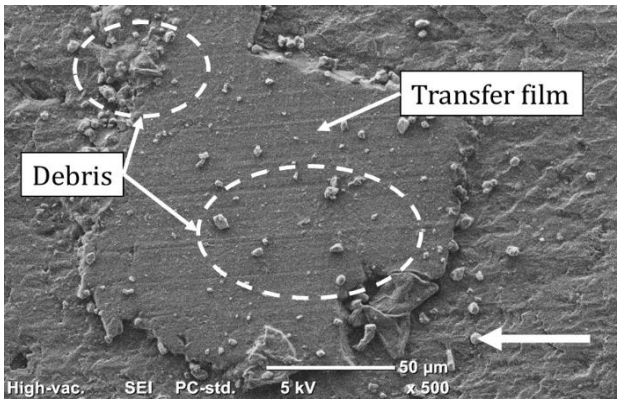

(d) Epoxy-Gr-9

Fig. 16. SEM images of the worn surfaces of epoxy-Gr composites at 30 N of applied load. The arrows on the bottom-right corner indicate the sliding direction of the ring.

The wear debris may act as abrasive particles at the beginning of the wear process, resulting in the three-body wear mechanism. However, during the wear process, the IFT increase leads to the wear debris' softening, creating a large and thick transfer film, as shown in Fig. 16 [d]. Therefore, adhesive wear is considered the predominant wear mechanism. However, the essential problem here is that the wear debris formation rate increases as the applied load increases. This could result in low transfer film stability and then accelerate the SWR values, as depicted in Fig. 8 [a and b]. As a result, the higher loads promoted the rate of material loss as wear debris, resulting in high SWR values. Similar observations were reported on other additives such as graphene oxide/epoxy composites [29], and graphene nanoplatelets/epoxy [11].

Surface roughness analysis is utilised to identify the impact of graphite addition and the applied loads on the roughness of the worn surfaces. Fig. 17(a) shows the effect of the applied loads on the roughness of the neat epoxy. It presents the Ra values obtained before and after the wear test. It is important to acknowledge that the surface roughness of the wear samples was prepared before the wear test to be less than 0.2 μm, as mentioned in Section 2.3. However, the applied load significantly impacted the surface roughness, especially at higher applied loads, where the roughness dramatically increased. For instance, the roughness dramatically increased by about 650% in the case of 70N. Although similar findings were spotted in all epoxy-Gr composites (not shown here), the reason behind each case was different. For neat epoxy, the reason is attributed to the high interface temperature that exceeded the HDT of epoxy in both cases of 50 N and 70 N.

Regarding epoxy-Gr composites, the reason could be attributed to the rapid rate of removing materials, producing massive wear debris, especially with a high concentration of graphite, as shown in Fig. 16(d). However, the presence of graphite exhibited a significant reduction in the roughness of the worn surface at lower concentrations of graphite. i.e., epoxy-Gr-3 composite, as shown in Fig. 17(b). Furthermore, at low applied loads (not shown here), all epoxy-Gr composites exhibited much less roughness change as compared to epoxy. This phenomenon can be attributed to the creation of transfer film, which covers the worn surface, reducing the surface roughness.

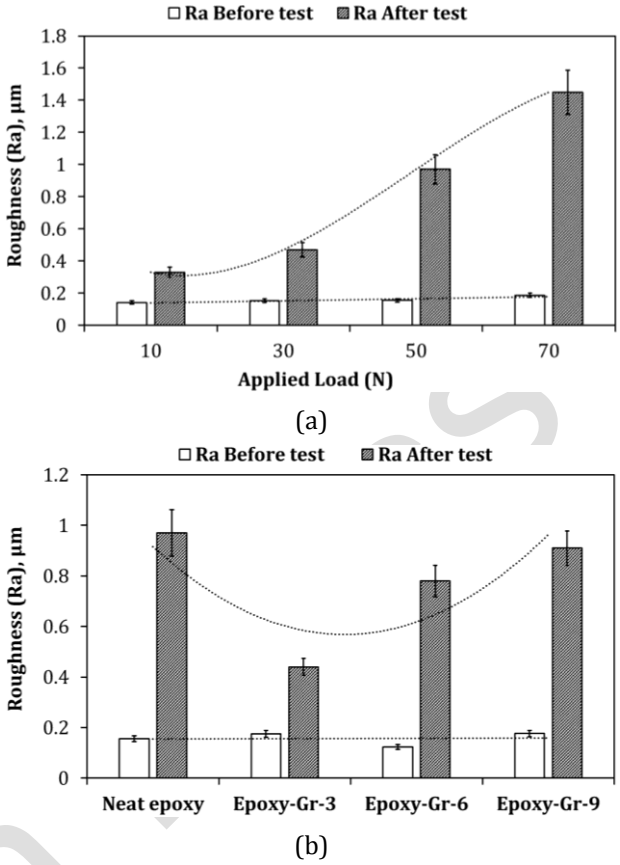

Fig. 17. Average surface roughness, Ra, before and after the wear test; (a) neat epoxy under all the applied loads and (b) epoxy-Gr composites under 50 N.

4. CONCLUSIONS

Epoxy composites were fabricated by including different weight percentages of graphite. The mechanical characteristics have been determined, and the wear and friction behaviours of the composites were investigated in a dry-wear environment. The loads were predetermined to encompass both the mild and severe regions, aiming to investigate the wear mechanisms that occur when IFT surpasses the HDT of epoxy. The investigation has yielded the following conclusions:

1. Graphite additions positively impacted both the elastic modulus and the hardness of epoxy. The increase in graphite concentration led to an increase in these properties.
2. On the other hand, graphite additions negatively impacted the fracture strength, fracture strain, and fracture toughness of epoxy. The higher the concentration in the graphite, the more reduction was observed.

3. In the mild wear region (10 to 30 N), the increase in graphite concentration significantly reduced the SWR of epoxy, where the maximum reduction was attained for epoxy-Gr-9 composite by 47% compared to neat epoxy. In contrast, in the severe wear region, the lowest graphite addition of 3 wt.% exhibited the lowest SWR value, as the higher concentrations of graphite additions showed a negative impact.
4. The graphite additions reduced the COF of epoxy due to its solid-lubrication properties. The maximum reduction is attained for epoxy-Gr-6 by about 41% as compared to the neat epoxy. Regarding the effect of applied loads, the increase in applied loads led to a decrease in the COF values for epoxy and its composites.
5. IFT is a significant factor in the wear process of epoxy. When it exceeds epoxy's HDT, SWR and COF dramatically increase. Herein, graphite additions de-accelerated the increase in IFT due to their ability to increase the TC of epoxy, thus enhancing the heat dissipation process.

Ultimately, this study suggests that the lower additions of graphite are more favourable to avoiding a negative alteration in the mechanical properties of epoxy, for instance, fracture strength and toughness. Regarding the tribological behaviour of epoxy, graphite as a solid lubricant additive exhibited a double-sided effect by reducing the COF and enhancing the heat dissipation process. It is highly recommended to use polymers that have a high HDT for such applications.

Acknowledgement

The author is highly grateful for the assistance from technicians and colleagues in the Centre of Future Materials (CFM), University of Southern Queensland (UniSQ), Australia

REFERENCES

[1] K. Friedrich, "Polymer composites for tribological applications," Advanced Industrial and Engineering Polymer Research, vol. 1, pp. 3-39, Oct. 2018, doi: 10.1016/j.aiepr.2018.05.001

[2] B.J. Briscoe, S.K. Sinha, "Tribological applications of polymers and their composites: past, present and future prospects," Tribology and interface engineering series, Elsevier, pp. 1–14, 2008, doi: 10.1016/S1572-3364(08)55001-4

[3] Y. Li, S. Wang, E. He, Q. Wang, "The effect of sliding velocity on the tribological properties of polymer/carbon nanotube composites," Carbon, vol. 106, pp. 106-109, Sep. 2016, doi: 10.1016/j.carbon.2016.04.077

[4] V. Kumar, S.K. Sinha, A.K. Agarwal, "Tribological studies of epoxy composites with solid and liquid fillers," Tribology International, vol. 105, pp. 27–36, Jan. 2017, doi: 10.1016/j.triboint.2016.09.010

[5] P.L. Menezes, P.K. Rohatgi, E. Omrani, Self-Lubricating Composites, Springer: Berlin/Heidelberg, Germany, 2022.

[6] M. Kalin, M. Zalaznik, S. Novak, "Wear and friction behaviour of poly-ether-ether-ketone (PEEK) filled with graphene, WS_2 and CNT nanoparticles," Wear, vol. 332, pp. 855-862, May-Jun. 2015, doi: 10.1016/j.wear.2014.12.036

[7] B. Ben Difallah, M. Kharrat, M. Dammak, G. Monteil, "Mechanical and tribological response of ABS polymer matrix filled with graphite powder," Materials & Design, vol. 34, pp. 782-787, Feb. 2012, doi: 10.1016/j.matdes.2011.07.001

[8] X. Zhang, G. Liao, Q. Jin, X. Feng, X. Jian, "On dry sliding friction and wear behavior of PPESK filled with PTFE and graphite," Tribology International, vol. 41, pp. 195-201, Mar. 2008, doi: 10.1016/j.triboint.2007.08.003

[9] K.E. Awwad, B. Yousif, A. Mostafa, O. Alajarmeh, X. Zeng, "Tribological and mechanical performances of newly developed eco-epoxy composites incorporating flax fibres and graphene nanoplatelets," Journal of Reinforced Plastics and Composites, vol. 42, pp. 939-952, Nov. 2023, doi: 10.1177/07316844221143451

[10] P.K. Bajpai, I. Singh, J. Madaan, "Tribological behavior of natural fiber reinforced PLA composites," Wear, vol. 297, pp. 829-840, Jan. 2013, doi: 10.1016/j.wear.2012.10.019

[11] K.Y. Eayal Awwad, B.F. Yousif, K. Fallahnezhad, K. Saleh, X. Zeng, "Influence of graphene nanoplatelets on mechanical properties and adhesive wear performance of epoxy-based composites," Friction, vol. 9, pp. 856-875, Feb. 2021, doi: 10.1007/s40544-020-0453-5

[12] I.O. Oladele, J.L. Olajide, M. Amujede, "Wear resistance and mechanical behaviour of epoxy/mollusk shell biocomposites developed for structural applications," Tribology in Industry, vol. 38, pp. 347-360, 2016.

[13] Y. Ye, J. Chen, H. Zhou, "An investigation of friction and wear performances of bonded molybdenum disulfide solid film lubricants in

fretting conditions," Wear, vol. 266, pp. 859–864, Mar. 2009, doi: 10.1016/j.wear.2008.12.012

[14] M.T. Masood, E.L. Papadopoulou, J.A. Heredia-Guerrero, I.S. Bayer, A. Athanassiou, L. Ceseracciu, "Graphene and polytetrafluoroethylene synergistically improve the tribological properties and adhesion of nylon 66 coatings," Carbon, vol. 123, pp. 26–33, Oct. 2017, doi: 10.1016/j.carbon.2017.07.026

[15] C. Pan, K. Kou, Y. Zhang, Z. Li, G. Wu, "Enhanced through-plane thermal conductivity of PTFE composites with hybrid fillers of hexagonal boron nitride platelets and aluminum nitride particles," Composites Part B: Engineering, vol. 153, pp. 1–8, Nov. 2018, doi: 10.1016/j.compositesb.2018.07.019

[16] F. Wang, L.T. Drzal, Y. Qin, Z. Huang, "Mechanical properties and thermal conductivity of graphene nanoplatelet/epoxy composites," Journal of Materials Science, vol. 50, pp. 1082–1093, Oct. 2015, doi: 10.1007/s10853-014-8665-6

[17] J.N. Panda, J. Bijwe, R.K. Pandey, "Role of treatment to graphite particles to increase the thermal conductivity in controlling tribo-performance of polymer composites," Wear, vol. 360–361, pp. 87-96, Aug. 2016, doi: 10.1016/j.wear.2016.04.018

[18] P. Li, Y. Zheng, M. Li, T. Shi, D. Li, A. Zhang, "Enhanced toughness and glass transition temperature of epoxy nanocomposites filled with solvent-free liquid-like nanocrystal-functionalized graphene oxide," Materials & Design, vol. 89, pp. 653–659, Jan. 2016, doi: 10.1016/j.matdes.2015.09.155

[19] ASTM D638-99, Standard Test Method for Tensile Properties of Plastics. ASTM International, West Conshohocken, PA, 2000.

[20] ASTM G77-98, Standard Test Method for Ranking Resistance of Materials to Sliding Wear Using Block-on-Ring Wear Test, ASTM International, West Conshohocken, PA, 1998.

[21] ASTM D2240, Standard Test Method for Rubber Property, ASTM International, West Conshohocken, PA, 2010.

[22] A.A. El-Sayed, M.G. El-Sherbiny, A.S. Abo-El-Ezz, G.A. Aggag, "Friction and wear properties of polymeric composite materials for bearing applications," Wear, vol. 184, pp. 45–53, Apr. 1995, doi: 10.1016/0043-1648(94)06546-2

[23] C.W. Chin, B.F. Yousif, "Potential of kenaf fibres as reinforcement for tribological applications," Wear, vol. 267, pp. 1550–1557, Sep. 2009, doi: 10.1016/j.wear.2009.06.002

[24] K.Y. Eayal Awwad, K. Fallahnezhad, B.F. Yousif, A. Mostafa, O. Alajarmeh, A. Shalwan, X. Zeng, "Finite element analysis and experimental validation of polymer–metal contacts in block-on-ring configuration," Friction, vol. 12, pp. 554-568, Dec. 2024, doi: 10.1007/s40544-023-0795-x

[25] M. Derradji, N. Ramdani, T. Zhang, J. Wang, T. Feng, H. Wang, W. Liu, "Mechanical and thermal properties of phthalonitrile resin reinforced with silicon carbide particles," Materials & Design, vol. 71, pp. 48–55, Apr. 2015, doi: 10.1016/j.matdes.2015.02.001

[26] A. Yasmin, I.M. Daniel, "Mechanical and thermal properties of graphite platelet/epoxy composites," Polymer, vol. 45, pp. 8211–8219, Nov. 2004, doi: 10.1016/j.polymer.2004.09.054

[27] J.A. Puértolas, M. Castro, J.A. Morris, R. Ríos, A. Ansón-Casaos, "Tribological and mechanical properties of graphene nanoplatelet/PEEK composites," Carbon, vol. 141, pp. 107–122, Jan. 2019, doi: 10.1016/j.carbon.2018.09.036

[28] J.A. Puértolas, S.M. Kurtz, "Evaluation of carbon nanotubes and graphene as reinforcements for UHMWPE-based composites in arthroplastic applications: A review," Journal of the Mechanical Behavior of Biomedical Materials, vol. 39, pp. 129–145, Nov. 2014, doi: 10.1016/j.jmbbm.2014.06.013

[29] Y. Li, R. Umer, A. Isakovic, Y.A. Samad, L. Zheng, K. Liao, "Synergistic toughening of epoxy with carbon nanotubes and graphene oxide for improved long-term performance," RSC advances, vol. 3, pp. 8849–8856, Mar. 2013, doi: 10.1039/c3ra22300k

[30] W. Qin, C. Chen, J. Zhou, J. Meng, "Synergistic effects of graphene/carbon nanotubes hybrid coating on the interfacial and mechanical properties of fiber composites," Materials, vol. 13, Mar. 2020, doi: 10.3390/ma13061457

[31] P.G. García, R. Ramírez-Aguilar, M. Torres, E.A. Franco-Urquiza, J. May-Crespo, N. Camacho, "Mechanical and thermal behavior dependence on graphite and oxidized graphite content in polyester composites," Polymer, vol. 153, pp. 9–16, Sep. 2018, doi: 10.1016/j.polymer.2018.06.069

[32] C. Salom, M.G. Prolongo, A. Toribio, A.J. Martínez-Martínez, I.A. de Cárcer, S.G. Prolongo, "Mechanical properties and adhesive behavior of epoxy-graphene nanocomposites," International Journal of Adhesion and Adhesives, vol. 84, pp. 119–125, Aug. 2018 doi: 10.1016/j.ijadhadh.2017.12.004

[33] R. Atif, I. Shyha, F. Inam, "Mechanical, thermal, and electrical properties of graphene-epoxy nanocomposites-A review," Polymers, vol. 8, Aug. 2016, doi: 10.3390/polym8080281

[34] S. Yu, H. Hu, J. Ma, J. Yin, "Tribological properties of epoxy/rubber nanocomposites," Tribology International, vol. 41, pp. 1205–1211, Dec. 2008, doi: 10.1016/j.triboint.2008.03.001

[35] E.I. Akpan, B. Wetzel, K. Friedrich, "A fully biobased tribology material based on acrylic resin and short wood fibres," Tribology International, vol. 120, pp. 381–390, Apr. 2018, doi: 10.1016/j.triboint.2018.01.010

[36] S.A.R. Hashmi, U.K. Dwivedi, N. Chand, "Graphite modified cotton fibre reinforced polyester composites under sliding wear conditions," Wear, vol. 262, pp. 1426–1432, May. 2007, doi: 10.1016/j.wear.2007.01.014

[37] J.D. Dotson, "The Effects of High Temperature on Epoxy," Sciencing, updated May 20, 2018. Available: Sciencing, https://sciencing.com/effects-high-temperature-epoxy-8590977.html. [Accessed Oct 10, 2023].

[38] S. Liu, C. Dong, C. Yuan, X. Bai, "Study of the synergistic effects of fiber orientation, fiber phase and resin phase in a fiber-reinforced composite material on its tribological properties," Wear, vol. 426–427, pp. 1047–1055, Apr. 2019, doi: 10.1016/j.wear.2018.12.090

[39] Z. Wang, R. Qi, J. Wang, S. Qi, "Thermal conductivity improvement of epoxy composite filled with expanded graphite," Ceramics International, vol. 41, pp. 13541–13546, `Dec. 2015, doi: 10.1016/j.ceramint.2015.07.148

[40] K. Friedrich, A.K. Schlarb, Tribology of polymeric nanocomposites: friction and wear of bulk materials and coatings, Elsevier; Butterworth-Heinemann, 2011.

[41] H.P. Arikh, P.P. Gohil, "Dry Sliding Wear Behavior of Pultruded Glass Fiber Epoxy Composites: Effect of Temperature," Materials Today: Proceedings, vol. 5, pp. 16453–16460, Aug. 2018, doi: 10.1016/j.matpr.2018.05.144

[42] N.A.M. Tahir, M.F. Bin Abdollah, R. Hasan, H. Amiruddin, "The effect of temperature on the tribological properties of palm kernel activated carbon-epoxy composite," Tribology Online, vol. 10, pp. 428–433, Dec. 2015, doi: 10.2474/trol.10.428

[43] C. Dong, L. Shi, L. Li, X. Bai, C. Yuan, Y. Tian, "Stick-slip behaviours of water lubrication polymer materials under low speed conditions," Tribology International, vol. 106, pp. 55-61, Feb. 2017, doi: 10.1016/j.triboint.2016.10.027